OPEN ACCESS
Jurnal Ilmiah Ilmu Terapan Universitas Jambi
Vol. 10 No. 1. Ferbruary 2026, pp. 255-267 DOI. 10.22437/jiituj.v10i1.50891
Research Article

MICROZONATION OF EARTHQUAKE HAZARD AREA USING THE HVSR METHOD IN THE SOUTHERN REGION OF KARANGASEM REGENCY

Nova Susanti[1,*], Rabiah Al Adawiyah[1], Febri Berthalita Pujaningsih[1], Alrizal[1], Athanasius Cipta[2]

[1] Physics Education Department, Universitas Jambi, Jambi, Indonesia
[2] Pusat Vulkanologi dan Mitigasi Bencana Geologi (PVMBG), Jawa Barat, Indonesia
Corresponding author email: nova_fisikaunja@unja.ac.id

Article Info
Received: Dec 06, 2025
Revised: Jan 09, 2026
Accepted: Feb 14, 2026
OnlineVersion: Feb 19, 2026

Abstract
Southern Karangasem Regency, Bali, is located in a tectonically active zone and requires detailed local scale earthquake hazard assessment. This study aims to develop an earthquake hazard microzonation map for Bungaya, Padang Kerta, Tiyingtali, and Ababi villages by integrating microtremor analysis and seismic source modeling. Single-station microtremor measurements were analyzed using the Horizontal-to-Vertical Spectral Ratio (HVSR) method to obtain dominant frequency (f_0), amplification factor (A_0), and seismic vulnerability index (K_g). Peak Ground Acceleration (PGA) was estimated based on modeled earthquake sources affecting the study area. The results show that f_0 values range from 0.51–8.78 Hz, A_0 values from 0.8–7.46, and K_g values from 0.78–14.86, indicating varying local site conditions. The estimated PGA ranges from 157 to 171 gals, corresponding to VI–VII on the MMI scale. The spatial distribution of these parameters reveals significant variation in earthquake hazard levels across the southern Karangasem region. The novelty of this study lies in the integration of HVSR-derived site response parameters with PGA modeling to produce a detailed village-scale microzonation map. The results provide valuable implications for seismic risk mitigation, spatial planning, and earthquake-resilient infrastructure development in seismically active regions.

Keywords: Earthquake Microzonation, HVSR Method, Karangasem Regency, Microtremor Analysis, Seismic Vulnerability Index, Peak Ground Acceleration.

INTRODUCTION

Indonesia is recognized as one of the most seismically active regions in the world due to its complex tectonic setting at the convergence of the Indo-Australian, Eurasian (Sunda), and Pacific plates. This triple-junction interaction generates intense seismicity, active volcanism, and frequent large megathrust earthquakes along the Indonesian archipelago (Hall, 2017; Widiyantoro et al., 2020). Geodetic and plate kinematic studies indicate that the Indo Australian Plate converges northward beneath the Sunda

Plate at rates of approximately 6–7 cm/year along the Sumatra–Java trench system, while the Pacific Plate and associated Philippine Sea Plate interact with eastern Indonesia at relative velocities reaching 8–11 cm/year, contributing to complex subduction, collision, and strike-slip faulting systems (Simons et al., 2016; Nugraha & Widiyantoro, 2019). In contrast, the Sunda (Eurasian) Plate exhibits comparatively slower internal deformation but plays a critical role as the overriding plate accommodating strain accumulation and release along major subduction zones.

The subduction of the Indo-Australian Plate beneath the Sunda margin extends from western Sumatra through southern Java, Bali, and Nusa Tenggara, forming one of the most seismically hazardous megathrust systems globally. Meanwhile, the tectonics of eastern Indonesia particularly the Maluku and Banda regions are dominated by complex interactions among the Eurasian, Pacific, and Philippine Sea plates, resulting in double subduction systems and highly heterogeneous seismic sources (Hall, 2017; Widiyantoro et al., 2020). This intricate plate configuration explains the high frequency of destructive earthquakes across Indonesia and underscores the necessity for detailed seismic hazard and microzonation studies.

Bali is one of the regions highly vulnerable to earthquake hazards because it is tectonically influenced by both the southern subduction zone and the northern back-arc thrust fault system (Ariyanto et al., 2024). Karangasem Regency, located in eastern Bali, lies close to these active tectonic structures, making its southern region particularly susceptible to tectonic earthquakes (Maryani, 2024). Historical seismic events confirm this vulnerability; for example, the January 2, 2004 earthquake caused casualties and severe damage to residential buildings, public facilities, and places of worship across Karangasem Regency. These impacts highlight that earthquake damage is not solely controlled by earthquake magnitude, but is strongly influenced by local site conditions and soil response characteristics.

Although earthquake occurrence cannot be prevented, its impacts can be significantly reduced through comprehensive mitigation strategies grounded in scientific assessment. One of the most essential approaches is seismic microzonation, which subdivides a region into smaller zones based on variations in local geological, geotechnical, and geophysical conditions that control ground motion amplification and site response characteristics. Seismic microzonation provides fundamental information for spatial planning, infrastructure design, and disaster risk reduction policies, particularly in rapidly urbanizing and seismically active regions (Pitilakis, 2018; Pagliaroli et al., 2021).

Among the various techniques applied in seismic microzonation, microtremor analysis has become widely adopted due to its practicality and efficiency. This method utilizes ambient ground vibrations generated by natural sources (e.g., oceanic microseisms, wind) and anthropogenic activities to infer subsurface dynamic properties without requiring invasive testing (Cox et al., 2020; Molnar et al., 2022). Microtremor recordings are commonly processed using the Horizontal-to-Vertical Spectral Ratio (HVSR) technique, which is recognized as a cost-effective, non-invasive, and environmentally friendly method suitable for dense urban environments (Lunedei & Albarello, 2019; Cheng et al., 2021).

HVSR analysis allows for the estimation of key site response parameters, including the dominant frequency (f_0), which reflects the fundamental resonance frequency of local soil layers, and the amplification factor (A_0), representing relative ground motion amplification. These parameters can further be used to estimate sediment thickness and compute the seismic vulnerability index (K_g), which indicates the susceptibility of near-surface deposits to seismic deformation (Tuan, 2019; Aini et al., 2021). Recent applications of HVSR-based microzonation in several urban regions of Indonesia and other seismically active countries have demonstrated its effectiveness in supporting urban planning, structural design considerations, and earthquake disaster mitigation frameworks (Marjiyono et al., 2020; Putra, 2022).

However, despite its high seismic potential, the southern region of Karangasem Regency has received limited attention in detailed seismic microzonation studies. The complex geological setting influenced by subduction processes, local faulting, and volcanic activity related to Mount Agung introduces significant spatial variability in site response that remains poorly characterized. This lack of site-specific information represents a critical research gap, particularly given the increasing exposure of residential areas and infrastructure in the region.

To address this gap, this study aims to develop a detailed seismic microzonation of southern Karangasem Regency using HVSR analysis of microtremor measurements. The research focuses on mapping the spatial distribution of dominant frequency (f_0), amplification factor (A_0), and seismic vulnerability index (K_g), integrated with Peak Ground Acceleration (PGA) estimates derived from earthquake source modeling. The novelty of this study lies in the application of an integrated, low-cost microzonation framework in a geologically complex and under investigated area of eastern Bali. The

results are expected to provide critical scientific insights and practical implications for earthquake risk mitigation, land use planning, and the development of earthquake-resilient infrastructure at the local scale.

RESEARCH METHOD

This study employed a quantitative observational geophysical survey with a descriptive analytical approach, aiming to characterize local site effects and seismic hazard through HVSR based microzonation. The research focuses on extracting subsurface dynamic properties from ambient noise measurements and integrating them with ground motion modeling to produce village-scale earthquake hazard maps. The study area covers the southern part of Karangasem Regency, Bali, including Bungaya, Padang Kerta, Tiyingtali, and Ababi villages, which are characterized by complex tectonic settings influenced by subduction, back-arc thrusts, and volcanic deposits. A total of 45 single station microtremor measurement points were deployed across the study area. Sampling locations were determined using a purposive spatial sampling technique, designed to represent variations in geology, geomorphology, land use, and settlement density. The number and distribution of stations satisfy commonly recommended criteria for HVSR based microzonation studies, which suggest dense spatial coverage to capture lateral variations in site response (SESAME, 2016).

Microtremor data were recorded using three-component seismometers capable of capturing vertical (Z), north–south (N–S), and east–west (E–W) ground motion components. Each recording lasted 20–30 minutes to ensure signal stability and adequate frequency resolution.

Tabel 1. Data acquisition followed international HVSR guidelines to minimize anthropogenic and transient noise effects

Parameter Measured	Instrument	Data Type	Output
Ambient vibration	3-component seismometer	Time series	Microtremor waveform
Horizontal motion	N–S, E–W channels	Frequency spectrum	H/V spectrum
Vertical motion	Z channel	Frequency spectrum	H/V spectrum

(SESAME, 2016).

Table 1. summarizes the data acquisition scheme implemented in this study, which follows internationally recognized HVSR measurement guidelines to minimize the influence of anthropogenic and transient noise during ambient vibration recording. Ambient vibrations were recorded using a three component seismometer, enabling simultaneous measurement of ground motion along the North–South (N–S), East–West (E–W), and vertical (Z) axes in the time domain. The acquired data consist of continuous microtremor time series, which are subsequently transformed into the frequency domain through spectral analysis. The horizontal components (N–S and E–W) are processed to obtain the horizontal motion spectrum, while the vertical component provides the reference vertical spectrum. These spectra are then combined to produce the Horizontal-to-Vertical Spectral Ratio (H/V spectrum), which characterizes site resonance frequency and amplification effects. Careful adherence to acquisition standards—including stable sensor installation, avoidance of cultural noise sources, and sufficient recording duration—is essential to ensure reliable HVSR interpretation (SESAME, 2016; Cox et al., 2020; Molnar et al., 2022). Recent studies emphasize that standardized acquisition protocols significantly improve the robustness and repeatability of HVSR results for seismic microzonation and site effect assessment (Lunedei & Albarello, 2019; Cheng et al., 2021).

Microtremor data processing in seismic site characterization commonly employs Geopsy software to analyze ambient vibration records and derive the Horizontal-to-Vertical Spectral Ratio (HVSR). Prior to spectral analysis, raw microtremor signals are pre processed to enhance data quality by removing transient noise and non stationary segments through visual inspection, signal quality control, and band pass filtering to retain the relevant frequency range (Cox et al., 2020; Molnar et al., 2022). After pre processing, a windowing procedure is applied by selecting multiple stationary windows commonly ten or more non overlapping segments with durations of 20 to 50 seconds, to ensure statistical stability and minimize contamination from transient disturbances (SESAME, 2016; Lunedei & Albarello, 2019). For each selected window, the horizontal components (North–South and East–West) are combined, and the spectral amplitudes of horizontal and vertical components are calculated using the Fast Fourier Transform (FFT). The HVSR curve is then obtained as the ratio between the averaged horizontal spectrum

and the vertical spectrum, revealing the dynamic characteristics of near-surface materials, particularly the site fundamental frequency and amplification effects (Cox et al., 2020).

From each resulting H/V curve, the dominant frequency (f_0) is identified as the principal spectral peak, representing the fundamental resonance frequency of the site, while the amplification factor (A_0) corresponds to the amplitude at that peak. These parameters are subsequently used to compute the seismic vulnerability index (Kg) following Nakamura's formulation, generally expressed as $Kg = \frac{A_0^2}{f_0}$. The Kg index provides an estimate of the susceptibility of near-surface soil layers to deformation under seismic loading, where high amplification and low dominant frequency values typically indicate softer sediments and greater vulnerability potential (Nakamura, 2014; Tuan, 2019; Aini et al., 2021). Consequently, integrating HVSR-derived parameters (f_0 and A_0) with the seismic vulnerability index enhances the interpretation of local site effects and supports seismic microzonation and disaster risk reduction strategies.

Peak Ground Acceleration (PGA) values in seismic hazard studies are commonly estimated using Ground Motion Prediction Equations (GMPEs), which are empirical models that relate earthquake source, path, and site characteristics to expected ground shaking intensity measures (e.g., PGA, spectral acceleration). In modern seismic hazard frameworks, GMPEs are integrated within tools such as OpenQuake Engine, enabling consistent implementation of multiple ground-motion models for probabilistic and deterministic hazard assessments (OpenQuake documentation, 2025). The selection and implementation of appropriate GMPEs involve parameters including moment magnitude, rupture distance metrics, fault geometry, hypocentral depth, and site conditions (e.g., Vs30), allowing for regionally calibrated estimates of PGA. This integrated approach enhances the physical realism of PGA calculations by accounting for both source physics and tectonic context, thus supporting more robust seismic hazard characterizations (Pagliaroli et al., 2021; OpenQuake documentation, 2025). In the present study, GMPE-based PGA estimation incorporated earthquake source parameters from the January 2, 2004 Karangasem earthquake, including magnitude and hypocentral distance, to derive a spatial representation of ground shaking intensity relevant for seismic microzonation and risk reduction planning. The flexibility of OpenQuake to test and combine multiple GMPE formulations further enables uncertainty analysis and comparison of ground-motion predictions under varying tectonic and site scenarios (Pagliaroli et al., 2021; Molnar et al., 2022).

The derived site response parameters, namely the dominant frequency (f_0), amplification factor (A_0), seismic vulnerability index (K_g), and Peak Ground Acceleration (PGA) were spatially interpolated using Geographic Information Systems (GIS) to generate high-resolution seismic microzonation maps at the village scale. Spatial interpolation techniques, such as kriging or inverse distance weighting (IDW), allow for the estimation of parameter values at unmeasured locations by leveraging spatial autocorrelation among observation points, thereby producing continuous surface maps that represent local variations in seismic response (Yilmaz et al., 2018; Singh et al., 2021). These microzonation maps delineate zones with differing susceptibility to seismic shaking, reflecting both geological heterogeneity and site amplification effects. Such maps serve as essential tools for evidence-based land-use planning, risk reduction, and earthquake-resistant infrastructure design, enabling authorities and engineers to prioritize areas for mitigation and resilient construction practices (Harb et al., 2020; Pagliaroli et al., 2021). Integrating geospatial analysis with HVSR derived parameters enhances the utility of seismic hazard assessments by providing spatially explicit information that can be directly applied to community planning and disaster management strategies.Statistical Analysis and Research Strength Statistical analysis focused on descriptive statistics (range, spatial distribution, and variability) of HVSR-derived parameters. Although inferential statistics are not the primary objective in site-response studies, the sample size of 45 measurement points provides adequate spatial resolution for microzonation at the village scale. According to previous HVSR studies, 30–50 stations are sufficient to reliably capture lateral site-response variability in small-to-medium-sized regions. Therefore, the dataset is considered statistically robust for identifying relative seismic hazard patterns, despite limitations in assessing nonlinear soil behavior.

RESULTS AND DISCUSSION

Dominant frequency (f_0), amplification factor (A_0), seismic vulnerability index (K_g), and Peak Ground Acceleration (PGA) values resulting from microtremor data processing are parameters in creating microzoning in the research area. Microzoning is the division of territory into several regions based on

differences in the potential for the impact of earthquake hazards. Microzonation maps can be used to determine the response and behavior of soil layers in the research area to earthquakes so that the results obtained by the microzonation map can be used as a mitigation effort against future disasters.

Dominant frequency value analysis (f_0)

Dominant frequency (f_0) is a fundamental parameter in seismic site characterization that reflects the resonant response between near-surface sediments and underlying bedrock (SESAME, 2004). It is strongly controlled by the effective shear-wave velocity and sediment thickness of the subsurface; specifically, thicker soft sediments tend to resonate at lower fundamental frequencies, while thinner sediment layers are associated with higher f_0 values (Iswanto et al., 2024). This inverse relationship arises because seismic waves propagating through deeper or softer materials require longer wavelengths and thus lower frequencies to resonate, whereas stiffer ground layers promote higher resonant peaks (Yang et al., 2025). Empirical and theoretical studies have demonstrated consistent correlations between HVSR-derived dominant frequency and sediment thickness, often expressed through simplified relationships such as $h = V_s/(4f_0)$, where $h$is the average sediment thickness and V_s is average shear-wave velocity (Iswanto et al., 2024; SESAME, 2004). Consequently, areas with low dominant frequency values generally indicate thick sediment deposits and potentially higher seismic site amplification, while high dominant frequency values suggest thin or stiff surface layers (Iswanto et al., 2024; Yang et al., 2025). In this study, dominant frequency values were obtained from HVSR analysis of microtremor records across the research area, and these values were classified according to rock and sediment types using a modified Kanai classification scheme, as summarized in Table 2.

Table 2. Classification of dominant frequency values

Land Classification		Dominant Classification (Hz)	Location
Class IV	Type I	6.667-20	
	Type II	4.0-10	MT26 MT30 MT45 MT1 MT3
Class III	Type III	2.5-4.0	
			MT2
Class II	Type IV	< 2.5	MT4-MT25
			MT27-MT29 MT31-MT44

Based on Table 2, the dominant frequency value (f_0) obtained in the research area is in the class IV and class II soil classifications. The range of dominant frequency values in class IV soil classification is between 4.55254 and 8.77978 Hz. This soil class is in 5 measurement locations out of the total 45 available, which locations are MT1, MT3, MT26, MT30, and MT45. Based on the classification by Kanai in Table 1, the type of soil in this area includes alluvial rock, with a thickness of 5 meters, consisting of sandy gravel, sandy hard clay, loam, and others. The range of dominant frequency values in class II soil classification is between 0.507872 – 2.24392 Hz spread over 40 measurement locations. It means that part of the research area is included in class II soil types. According to Kanai's classification in Table 2, the types of soil that are generally distributed in this area indicate alluvial rocks formed from delta sedimentation, topsoil, mud, and others with a depth of 30m or more. The distribution of each dominant frequency value in the research area can be seen on the contour map as follows:

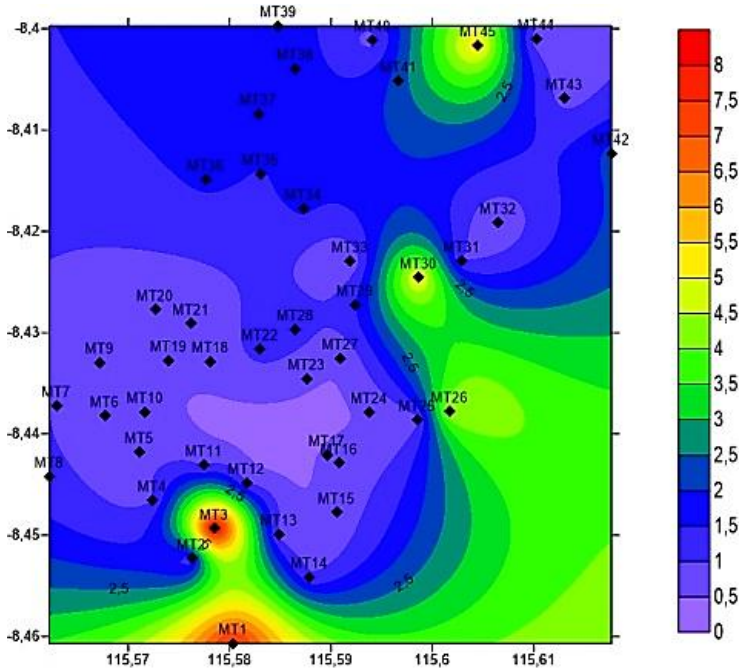

Figure 1. Contour map of the distribution of dominant frequency values (f_0)

In Figure 1, the dominant frequency values across the study area vary from 0.51 to 8.78 Hz, with the majority of locations exhibiting relatively low frequencies (represented by purple to blue hues). Low dominant frequency values typically indicate the presence of soft, thick sedimentary deposits with lower shear-wave velocities, which are known to amplify seismic shaking (Iswanto et al., 2024). This is consistent with the principle that sites underlain by deeper, softer sediments tend to resonate at lower frequencies and may experience enhanced ground motion during earthquakes (SESAME, 2016). In seismic microzonation studies, such areas are often associated with higher amplification potential and increased seismic risk, particularly for structures with natural frequencies that match the prevailing site frequencies (Bommer & Akkar, 2016).

In the northern portion of the research area, where dominant frequencies remain low, there is a greater likelihood of significant ground motion amplification and potentially more severe earthquake effects. Empirical investigations have shown that regions characterized by low f_0 values frequently correspond to greater structural damage and higher seismic vulnerability in past earthquake events (Wang & Wang, 2023; Yang et al., 2025). Therefore, these low-frequency zones warrant particular attention in risk mitigation planning and infrastructure design.

Analysis of amplification factor values (A0)

The amplification factor (A_0) quantifies the degree to which seismic wave amplitudes increase as they propagate from bedrock into overlying soil layers with contrasting mechanical properties. Amplification occurs because seismic waves interacting with softer, lower-velocity sediments slow down and their amplitudes increase to conserve energy, a phenomenon widely recognized as site amplification (SESAME, 2016). In simple physical terms, when vertically propagating shear waves encounter a soil layer with significantly lower stiffness than the underlying material, the impedance contrast results in increased ground motion at the surface.

Recent experimental and modeling studies confirm that softer and thicker sedimentary deposits produce higher amplification factors relative to stiffer or thinner soils (Kusuma, 2024; Yang et al., 2025). These effects are not purely a function of layer softness, but also of thickness, velocity gradient, and geometry of layering, which together influence the resonance characteristics of the site (Yang et al., 2025). Amplification is often more pronounced in valley or basin settings where low-velocity sediments trap seismic energy and lead to extended shaking durations and larger amplitudes (Marasabessy et al., 2025). Therefore, areas underlain by soft sediments such as hilly valleys or basins are typically associated with increased seismic hazard and higher potential for structural damage due to amplified ground motion when compared to regions with competent bedrock.The value of the amplification factor is influenced by the wave speed. If the wave speed is smaller, the amplification factor will be bigger. It shows that the

amplification factor is related to the level of rock density, where reducing rock density will increase the value of the amplification factor. In addition, the value of the soil strengthening factor relates to the impedance contrast of the surface layer with the layer beneath it. If the comparison of the impedance contrast between the two layers is high, the value of the strengthening factor is also high, and vice versa (Nakamura, 2014). The amplification factor values in the research area vary, with low, medium, and high values. The results of the amplification factor values obtained can be classified into three zones, which are in the following Table 3.

Table 3. Classification of amplification factor values

Classification	Amplification Factor	Location
Low	A < 3	MT5-MT7 MT9 MT10 MT13 MT15-MT25 MT27-MT29 MT31-MT33 MT35 MT37-MT41 MT43-MT45
Moderate	3 ≤ A < 6	MT1 MT2 MT4 MT8 MT11 MT12 MT14 MT26 MT30 MT34 MT36 MT42
High	6 ≤ A < 9	MT3

Based on Table 3, the amplification factor values in the research area are divided into three classification zones, which are low, medium, and high. The low zone is less than three based on microtremor data processing. This low zone is found at 32 measurement locations in the research area. The range of amplification factor values obtained is between 0.802337 – 2.94254. Medium zone with amplification factor value classification from 3 to 6 spread over 12 measurement locations, namely MT1, MT2, MT4, MT8, MT11, MT12, MT14, MT26, MT30, MT34, MT36, and MT42 with amplification factor values obtained from analysis microtremor data ranges from 3.0481 – 5.85431. The high zone classification is only at one measurement location, which is MT3, with an amplification factor value of 7.46076. To find out the distribution of amplification factor values in the research area, below is the map:

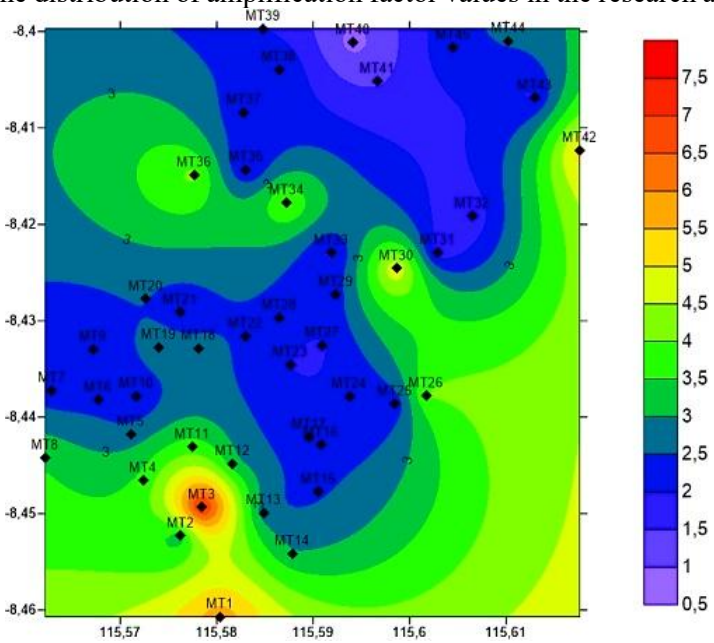

Figure 2. Contour map of the distribution of amplification factor values

Based on Figure 2, the overall range of amplification factor values in the research area ranges from 0.802337 to 7.4607. According to Nakamura (2014) the amplification parameter can damage buildings if the value is greater than three and is associated with low frequencies. Based on the contour map in Figure 2, amplification factor values of more than three are marked in dark green to red in the southern part, and a small portion is colored green in the northwestern part of the research area. Therefore,

this area tends to get large strengthening and result in damage when an earthquake occurs. Low amplification factor values dominate in the research area, which is marked with purple to blue colors at 31 measurement locations. In research conducted by Daryono et al., the amplification factor value was correlated with the damage ratio value. The area with maximum damage had a large amplification factor value and vice versa (Brotopuspito, 2016). Research areas that have low amplification factor values are classified as safe areas.

Seismic vulnerability index value analysis (Kg)

The seismic vulnerability index value (K_g) is a value obtained from two previously generated parameters, which are the dominant frequency value and the amplification factor value. Calculation of the seismic vulnerability index (Kg). The seismic vulnerability index (Kg) value can describe the level of vulnerability of an area to seismic waves. The seismic vulnerability index value is used to identify an area that is vulnerable to strong ground movement (Brotopuspito, 2016). The seismic vulnerability index value can be used to determine the potential for an area to experience damage due to an earthquake. The seismic vulnerability index value obtained from calculating the dominant frequency value and amplification factor has varying values ranging from low, medium, and high. The distribution of seismic vulnerability index values in the research area is in the following Table 4.

Table 4. Seismic vulnerability index value (K_g)

Classification	Seismic Vulnerability Index (K_g)	Location
Low	< 3	MT39-MT41 MT45 MT35 MT37
Moderate	3-6	MT26 MT1 MT43 MT22 MT7 MT25 MT3 MT38 MT28-MT32
High	> 6	MT2 MT4 MT5 MT6 MT8-MT21 MT23 MT24 MT33 MT34 MT36 MT27 MT42 MT44

Based on Table 4, the seismic vulnerability index values in the research area are in 3 zones, which are classified based on the vulnerability of the soil in resisting seismic waves. The low zone is at a seismic vulnerability index value of less than three at six measurement locations, namely MT39, MT40, and MT41. MT45, MT35, and MT37. The zone with a moderate level of vulnerability is at values 3 – 6, which are at 13 measurement locations, namely MT26, MT1, MT43, MT22, MT7, MT25, MT3, MT38, MT28, MT29, MT30, MT31, and MT32. Zones with a high level of vulnerability are in most of the research area, which is at 26 measurement locations that have a value of more than 6, namely at MT2, MT4, MT5, MT6, MT8, MT9, MT10, MT11, MT12, MT13, MT14, MT15, MT16, MT17, MT18, MT19, MT20, MT21, MT23, MT24, MT33, MT34, MT36, MT27, MT42 and MT44. The distribution of seismic vulnerability index (Kg) values at the research location is in the following contour map:

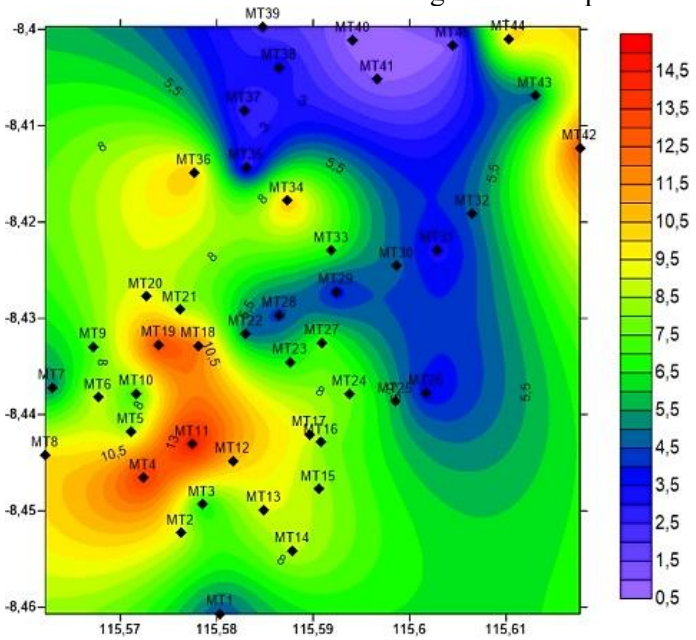

Figure 3. Contour map of the distribution of seismic vulnerability index values (K_g)

Figure 3 is a contour map of the distribution of seismic vulnerability index values in the research area. The seismic vulnerability index value is in the range 0.777364 – 14.86166, which is marked in purple to red. The seismic vulnerability index value is influenced by the value of the amplification factor. In which areas with high amplification factor values will have a large seismic hazard vulnerability value. The seismic vulnerability index values in the research area appear to vary even though they are in the same geological conditions. According to Septian, the seismic vulnerability index value is directly proportional to the damage to buildings caused by earthquakes (Douglas, 2018). The higher the vulnerability index value of an area, the greater the danger level posed by an earthquake disaster.

The seismic vulnerability index value of the research area, which is at a high hazard level, is at a value of 6.637618 – 14.86166 with a light green to red. From the administrative location, the areas with a high vulnerability index value are in the southern region, which includes Bungaya Village, Padang Kerta, and parts of Ababi. Meanwhile, areas with a low seismic hazard level are in the value range between 3.141768 and 6.339901, shown in light blue to dark green. Administratively, the areas with low seismic hazard are in the northern part of the research area, namely Tiyingtali Village and parts of Ababi. Based on the microzonation map, the seismic vulnerability index value of areas that are at a high hazard level should receive special attention, namely by building buildings that meet the requirements of earthquake-resistant buildings. This step can be an effort to minimize the danger of damage due to earthquakes.

Peak Ground Acceleration (PGA) value analysis

Peak Ground Acceleration (PGA), also referred to as maximum ground acceleration, represents the maximum value of ground acceleration recorded at a site during an earthquake and is widely used as a key parameter for characterizing seismic ground motion severity (Douglas, 2018). PGA reflects the combined influence of earthquake source characteristics, propagation path, and local site conditions, and is therefore essential for seismic hazard assessment and engineering design. In this study, PGA values were obtained through earthquake source modeling based on the Karangasem earthquake that occurred on January 2, 2004, with a moment magnitude of Mw 6.2 and an epicenter located at 115.79° E longitude and 8.26° S latitude.

The PGA estimation was performed using ground motion prediction equations (GMPEs), which relate earthquake magnitude, source-to-site distance, and fault parameters to expected ground acceleration levels (Douglas, 2018). The resulting PGA values across the study area range from 157 to 171 gal, indicating moderate to strong ground shaking. When correlated with the Modified Mercalli Intensity (MMI) scale, these PGA values correspond predominantly to intensity levels VI–VII, which are commonly associated with slight to moderate structural damage, particularly in buildings constructed on soft soil deposits (Muzli et al., 2016). The spatial distribution of PGA suggests that most areas within the southern Karangasem region fall within the MMI VI category, emphasizing the importance of incorporating PGA-based hazard information into seismic microzonation, land-use planning, and earthquake-resilient infrastructure development.

Table 5. Peak Ground Acceleration (PGA) value

MMI Scale	PGA (gal)	Location
VI	89 - 167	MT1-MT29 MT31-MT39 MT43 MT44 MT45
VII	168 - 564	MT30 MT40 MT41 MT42

Based on Table 5, the PGA value on the VI MMI scale is 89-167 gal spread across 41 measurement locations, so the research area is included in the danger of experiencing light damage (slight damage). In detail, areas with a VI MMI scale will cause non-structural parts of the building to experience minor damage, such as hairline cracks on the walls, the roof shifting downwards, and parts falling. Furthermore, areas with a PGA value on the VII MMI scale in the range of 168-564 gal spread over four measurement locations are considered to be in danger with moderate damage. In detail, areas with a PGA value on the VII MMI scale will have many cracks in the walls of simple buildings, some collapse, and glass breaking. As well as some of the wall plaster coming off and most of the roof sliding down or falling, the building suffered light to moderate damage. The distribution pattern of earthquake hazards based on PGA values can be determined using a microzonation map. The microzonation map of maximum ground acceleration values is in the following contours:

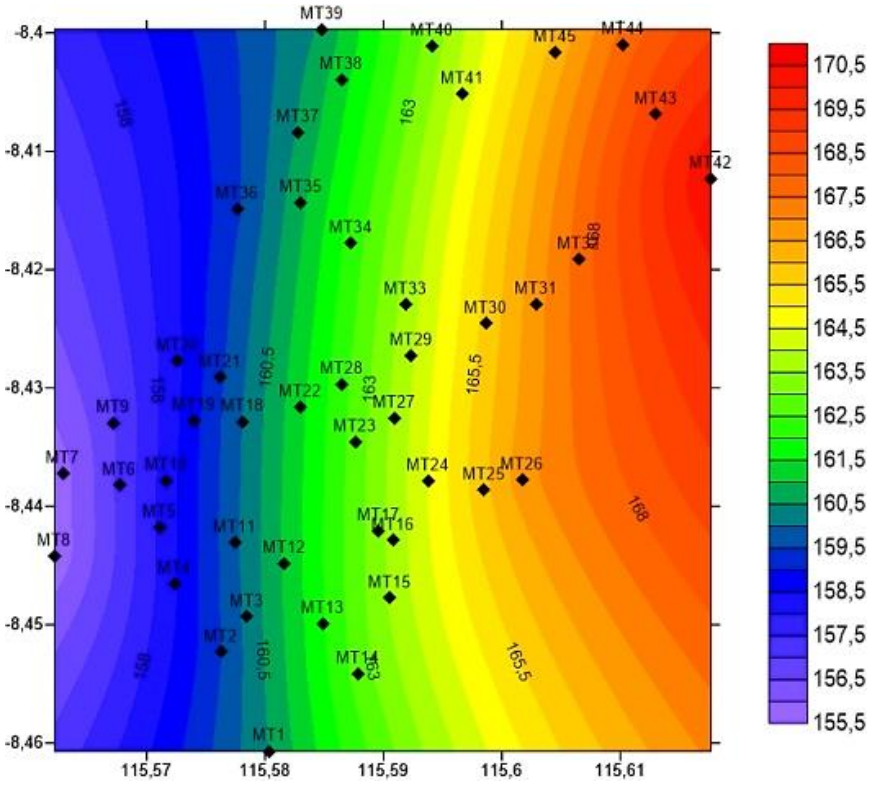

Figure 4. Contusion map of Peak Ground Acceleration (PGA)

Based on the contour map of maximum ground acceleration values in Figure 4, the research area is between 156.5 and 170.5 gal. The highest maximum ground acceleration value in the research area is at coordinates 115.61765 East Longitude and -8.41232 South Latitude in Ababi Village. Meanwhile, the maximum ground acceleration value is at 115.56718 East Longitude and -8.43294 South Latitude in Bungaya Village. The maximum ground acceleration value on the VI MMI scale is in the range of values between 157 and 167 gal. This value is spread throughout the research area evenly in the western part. Meanwhile, the highest maximum ground acceleration values ranging from 167 to 168 gal are in the eastern part of the research area. The distribution of maximum ground acceleration values in general in the research area, is dominated by the PGA value on the VI MMI scale, which in detail, when an earthquake occurs, buildings will experience minor damage, such as cracks forming hairs on the walls, roofs shifting downwards and some falling.

A microzonation map of the research area can be created based on the maximum ground acceleration distribution values. The microzonation map depicts the level of vulnerability of the research area to earthquake disasters. Additionally, the distribution map of maximum ground acceleration values can also be used as a study and information in designing a building. According to Hadi, this maximum ground acceleration map is one of the guidelines for spatial and regional planning (RT RW), which can provide recommendations for the placement of residential buildings and other vital buildings in areas where the potential for maximum ground acceleration is low (Brotopuspito, 2016).

This study demonstrates that HVSR-based microzonation is an effective approach for identifying spatial variations in local site response in the southern region of Karangasem Regency. The resulting microzonation maps provide clear evidence of heterogeneous seismic vulnerability, reflecting the influence of local geological and sedimentary conditions. These findings strengthen the understanding that local site effects play a critical role in earthquake damage distribution, even within relatively small geographic areas.

The results offer practical implications for earthquake risk mitigation and disaster preparedness, particularly for regional authorities responsible for spatial planning and infrastructure development. By identifying zones with higher amplification and seismic vulnerability, this research contributes to the development of risk-sensitive land-use policies and building design considerations, especially in tectonically active regions such as eastern Bali. Moreover, the methodological framework presented in this study can serve as a reference for similar microzonation studies in other regions characterized by limited instrumental seismic data.

Limitations of the Research, While the HVSR method provides valuable insight into site response characteristics, this study is subject to several limitations that should be considered when interpreting the results. The analysis is based on ambient noise measurements, which primarily capture linear soil behavior and may not fully represent site response under strong earthquake loading. In addition, the lack of borehole data and direct shear-wave velocity measurements constrains the ability to validate subsurface models and to quantify non-linear soil effects. Furthermore, the seismic hazard interpretation relies on empirical ground motion models, which may not fully account for local source and path effects specific to the Karangasem region. Therefore, the microzonation results should be regarded as a preliminary but essential baseline for seismic risk assessment. Future studies are encouraged to integrate HVSR analysis with geotechnical investigations, Vs profiling, and strong-motion observations to enhance the robustness and applicability of seismic microzonation in the study area.

CONCLUSION

This research confirms the effectiveness of the HVSR method for seismic microzonation in the southern part of Karangasem Regency, demonstrating pronounced spatial variations in local site response influenced by geological and sedimentary conditions. The microzonation analysis identifies areas characterized by elevated amplification and dominant frequencies, indicating higher potential seismic vulnerability and reinforcing the critical role of local site effects in earthquake hazard evaluation. The results serve as an important baseline for seismic risk reduction, land-use planning, and the development of earthquake-resistant infrastructure in eastern Bali, a region with high tectonic activity and limited strong-motion observations. The analysis shows that the dominant frequency (f_0) across the study area varies between 0.50787 and 8.77978 Hz, with spatial distribution observed throughout the region. Amplification factors (A_0) range from 0.802337 to 7.46076, suggesting generally low to moderate amplification levels. The seismic vulnerability index values vary from 0.77736 to 14.86166, while peak ground acceleration (PGA) values range from 157 to 171 gal, corresponding to intensity levels of VI–VII on the MMI scale. Areas with relatively higher earthquake hazard are identified in Bungaya Village, Padang Kerta, and parts of Ababi. The highest estimated maximum ground acceleration is located in Ababi Village at coordinates 115.6175°E and 8.41232°S. Despite its effectiveness in capturing linear site response using ambient noise, the absence of borehole data, shear-wave velocity profiles, and strong-motion records limits the evaluation of non-linear soil behavior, indicating the need for integrated geotechnical and ground motion studies in future research.

ACKNOWLEDGMENTS

The author team would like to thank the Center for Volcanology and Geological Disaster Mitigation (PVMBG) for the opportunity to directly learn about data and data processing and to learn more about earthquakes.

AUTHOR CONTRIBUTIONS

Author one: conceptualization, methodology, writing original draft preparation, review and editing, administration, funding acquisition; Author two: Software, data curation, writing original draft preparation; Author three: formal analysis, supervision, methodology.

CONFLICTS OF INTEREST

The author(s) declare no conflict of interest.

USE OF ARTIFICIAL INTELLIGENCE (AI)-ASSISTED TECHNOLOGY

The authors declare that no artificial intelligence (AI) tools were used in the generation, analysis, or writing of this manuscript. All aspects of the research, including data collection, interpretation, and manuscript preparation, were carried out entirely by the authors without the assistance of AI-based technologies.

REFERENCES

Aini, N., Fathani, T. F., & Wilopo. (2021). Seismic vulnerability assessment based on HVSR method for site effect evaluation. *Indonesian Journal of Geoscience, 8*(2), 123–134.

Ariyanto, D., Nugraha, J., Sunardi, B., & Widiyantoro, S. (2024). Seismic hazard assessment of Bali Island based on tectonic setting and recent seismicity. *Journal of Asian Earth Sciences, 248*,

105796. https://doi.org/10.1016/j.jseaes.2023.105796.
Bommer, J. J., & Akkar, S. (2016). Long-period microtremor H/V spectral peaks: A physical background and engineering significance. *Earthquake Spectra, 32*(4), 1911–1923. https://doi.org/10.1193/061915EQS186M.
Brotopuspito, K. S. (2016). *Percepatan getaran tanah maksimum di Indonesia*. HAGI.
Cheng, T., Cox, B. R., & Vantassel, J. P. (2021). Influence of field acquisition parameters on HVSR measurements for site characterization. *Bulletin of the Seismological Society of America, 111*(3), 1467–1483.
Cox, B. R., Cheng, T., & Vantassel, J. P. (2020). A statistical representation and frequency-domain window-rejection algorithm for single-station HVSR measurements. *Bulletin of the Seismological Society of America, 110*(4), 1900–1915.
Douglas, J. (2018). Ground motion prediction equations 1964–2018. *Earthquake Spectra, 34*(4), 1781–1805. https://doi.org/10.1193/060418EQS133M.
Hall, R. (2017). Southeast Asia: New views of the geology of the Malay Archipelago. *Annual Review of Earth and Planetary Sciences, 45*, 331–358. https://doi.org/10.1146/annurev-earth-063016-020633.
Harb, S., Al-Atik, L., & Biondi, B. (2020). GIS-based seismic microzonation incorporating HVSR and site amplification: Applications for urban planning. *Earthquake Spectra, 36*(2), 667–690. https://doi.org/10.1177/8755293020918586.
Irsyam, M., Widiyantoro, S., Natawidjaja, D. H., Meilano, I., Rudyanto, A., Hidayati, S., & Triyoso, W. (2017). Development of the 2017 national seismic hazard maps of Indonesia. *Earthquake Spectra, 33*(S1), 1–25. https://doi.org/10.1193/052017EQSpectra.
Iswanto, E. R., Riyanto, T. A., & Suntoko, H. (2024). Relationship between HVSR dominant frequency and sediment thickness in West Nusa Tenggara, Indonesia. *Eksplorium, 44*(2), 57–66. https://doi.org/10.55981/eksplorium.2023.8171.
Kusuma, A. (2024). Microtremor analysis and seismic vulnerability distribution in Muara Aman, Lebong Regency. *Jurnal Fisika, 14*(2), 39–45.
Lunedei, E., & Albarello, D. (2019). On the reliability of HVSR measurements and interpretation in seismic microzonation. *Soil Dynamics and Earthquake Engineering, 120*, 274–286.
Marasabessy, M. I., Saputra, E., & Basarah, Y. I. (2025). Evaluation of seismic site amplification factors in Yogyakarta using one-dimensional site response analysis. *Teknisia, 30*(1), 1–12. https://doi.org/10.20885/teknisia.vol30.iss1.art1.
Marjiyono, M. (2020). Application of microtremor HVSR method for seismic microzonation in urban areas of Indonesia. *IOP Conference Series: Earth and Environmental Science, 469*, 012031.
Maryani, S. (2024). Geological structure and seismic risk of eastern Bali region. *Indonesian Journal of Geoscience, 11*(2), 89–102.
Molnar, S., Cassidy, J. F., & Dosso, S. E. (2022). Advances in ambient noise HVSR processing for site response analysis. *Seismological Research Letters, 93*(5), 2754–2766.
Muzli, M., Masturyono, M., Murjaya, J., & Riyadi, M. (2016). Preliminary study on the development of an earthquake intensity scale for Indonesia. *Jurnal Meteorologi dan Geofisika, 17*(2), 89–98. https://doi.org/10.31172/jmg.v17i2.440.
Nakamura, Y. (2014). On the H/V spectrum. *Proceedings of the International Symposium on the Effects of Surface Geology on Seismic Motion*, 1–12.
Nugraha, A. D., & Widiyantoro, S. (2019). Active tectonics and seismicity of the Indonesian region from integrated geophysical observations. *Geoscience Letters, 6*(1), 1–15.
OpenQuake documentation. (2025). *Ground motion prediction equations—OpenQuake Engine manual*. https://docs.openquake.org/oq-engine/latest/manual/underlying-science/gmpes.html
Pagliaroli, A., Pitilakis, K., & Crowley, H. (2021). Seismic microzonation: Advances and perspectives. *Soil Dynamics and Earthquake Engineering, 149*, 106850. https://doi.org/10.1016/j.soildyneng.2021.106850.
Pitilakis, K. (2018). Recent advances in seismic microzonation studies and applications. *Bulletin of Earthquake Engineering, 16*, 1–38.
Putra, R. R. (2022). Microtremor-based site response analysis for urban seismic hazard assessment in Indonesia. Indonesian Journal of Physics, 33(1), 45–56.
Rohadi, S., Taruna, R. M., Rudyanto, A., & Heryanto, D. T. (2016). Determination of ground motion prediction equations using Euclidean and likelihood methods in Java. *Journal of Meteorology*

and Geophysics, 17(3), 141–150. https://doi.org/10.31172/jmg.v17i3.357.

SESAME European Research Project. (2016). *Guidelines for the implementation of the H/V spectral ratio technique on ambient vibrations: Measurements, processing and interpretation*. European Commission.

Simons, W. J. F., Socquet, A., Vigny, C., Ambrosius, B. A. C., Haji Abu, S., Promthong, C., Subarya, C., Sarsito, D., Matheussen, S., Morgan, P., & Spakman, W. (2016). A decade of GPS in Southeast Asia: Resolving Sundaland motion and boundaries. *Journal of Geophysical Research: Solid Earth, 121*(2), 1219–1232.

Singh, A., Rai, D. C., & Saha, S. (2021). Spatial interpolation of geotechnical parameters for seismic microzonation using GIS: A comparative study of kriging and IDW approaches. *Journal of Earthquake Engineering, 25*(5), 765–788. https://doi.org/10.1080/13632469.2020.1844205.

Sunardi, B., & Nugraha, J. (2016). Peak ground acceleration and spectral acceleration based on probabilistic seismic hazard analysis. *Journal of Meteorology and Geophysics, 17*(1), 23–34. https://doi.org/10.31172/jmg.v17i1.380.

Tuan, T. A. (2019). Application of HVSR method for seismic vulnerability index and microzonation study. Engineering Geology, 259, 105–113.

Wang, Z., & Wang, H. (2023). Influence of site response characteristics on seismic damage distribution: Insights from microtremor analysis. *Journal of Seismology and Earthquake Engineering, 25*(5), 301–316. https://doi.org/10.1007/s10950-023-10044-7.

Widiyantoro, S., Nugraha, J., & Irsyam, M. (2020). Seismotectonics of Indonesia: Implications for seismic hazard assessment. *Geological Society, London, Special Publications, 501*, 1–18. https://doi.org/10.1144/SP501-2019-101.

Yang, Y., Shi, L., & Huang, J. (2025). Spatial variability of HVSR dominant frequency for seismic microzonation: Case studies in Eastern Asia. *Discover Geoscience, 3*, 73. https://doi.org/10.1007/s44288-025-00185-8.

Yilmaz, I., Duman, T. Y., & Nalbant, S. S. (2018). GIS-based seismic hazard mapping using HVSR and geostatistical interpolation: Case study and implications. *Bulletin of Earthquake Engineering, 16*, 305–323. https://doi.org/10.1007/s10518-017-0279-7.